

Supporting Information

A New Indium Selenide Phase: Controllable Synthesis, Phase Transformation and Photoluminescence Properties†

Guang Han,^{*a,b} Qinfen Gu,^c Lei Yang,^d Zhi-Gang Chen,^{*e,b} and Jin Zou^{*b,f}

^a College of Materials Science and Engineering, Chongqing University, Chongqing 400044, China;

Email: guang.han@cqu.edu.cn

^b Materials Engineering, The University of Queensland, Brisbane, Queensland 4072, Australia;

Email: j.zou@uq.edu.au

^c Australian Synchrotron (ANSTO), Clayton, Victoria 3168, Australia

^d School of Materials and Science Engineering, Sichuan University, Chengdu 610065, China

^e Centre for Future Materials, University of Southern Queensland, Springfield Central, Queensland 4300, Australia

Email: zhigang.chen@usq.edu.au

^f Centre for Microscopy and Microanalysis, The University of Queensland, Brisbane, Queensland 4072, Australia

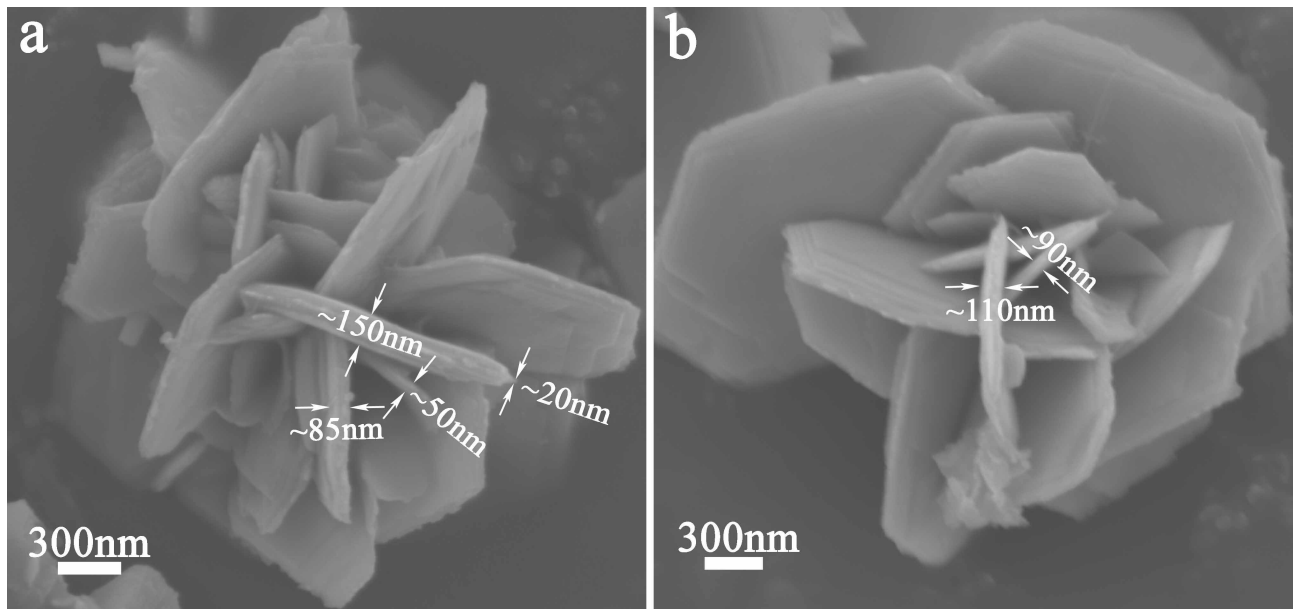


Fig. S1 SEM images of $\text{In}_{2.45}\text{Se}_4$ flowerlike nano/microstructures revealing the thickness of plates.

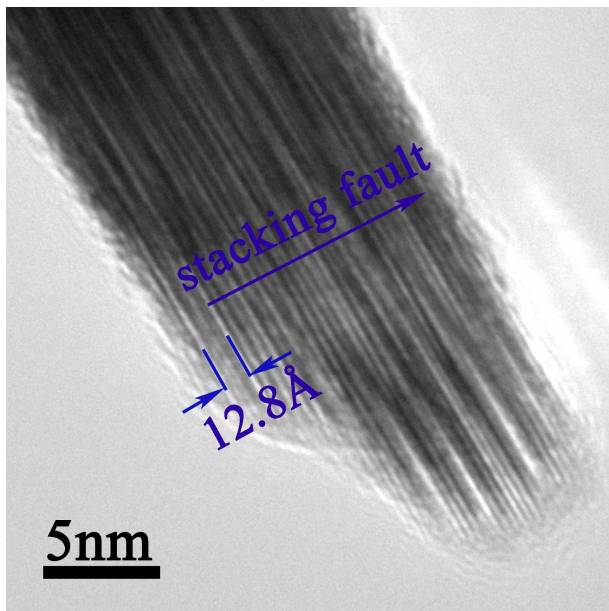


Fig. S2 HRTEM image of $\text{In}_{2.45}\text{Se}_4$ nanoplate viewing along the nanoplate surface.

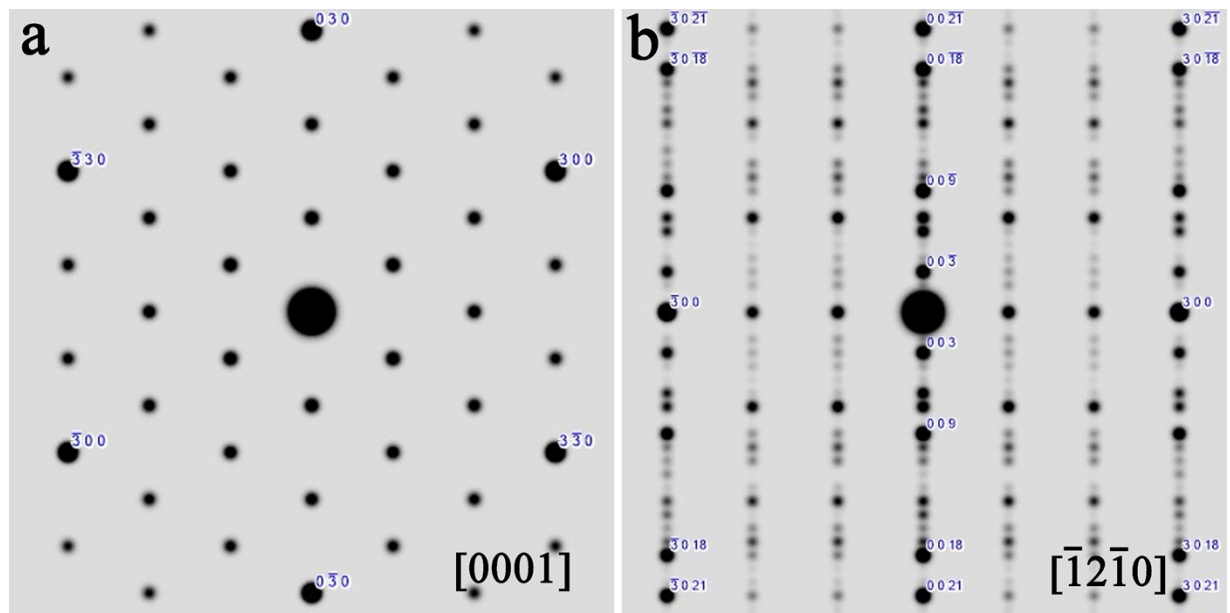


Fig. S3 Simulated SAED patterns of the new phase along (a) $[0001]$ and (b) $[\bar{1}2\bar{1}0]$ zone-axis, respectively.

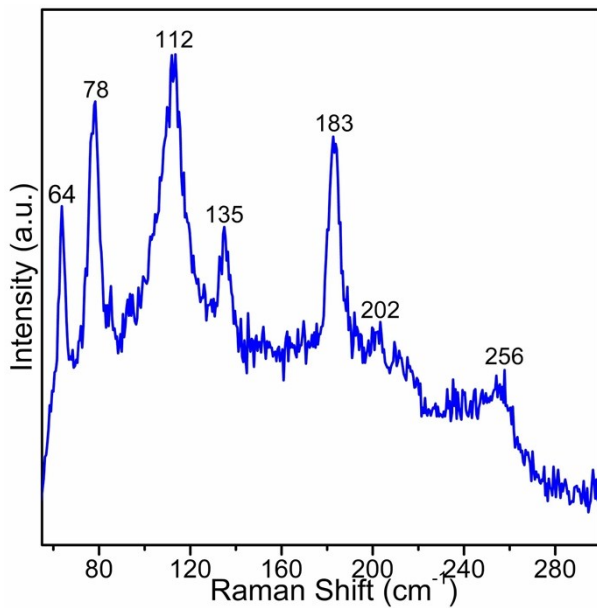


Fig. S4 Raman spectrum of $\text{In}_{2.45}\text{Se}_4$ flowerlike nano/microstructures.

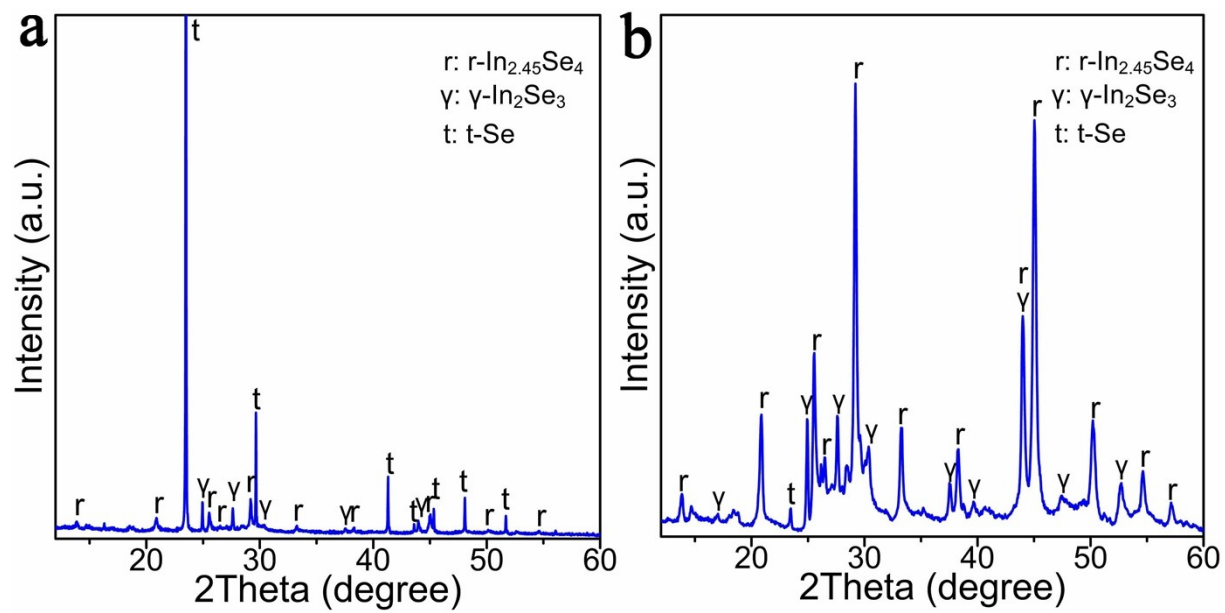


Fig. S5 Lab-based PXRD patterns (Cu K α radiation) of products synthesized at different temperatures: (a) 200 °C, (b) 230 °C.

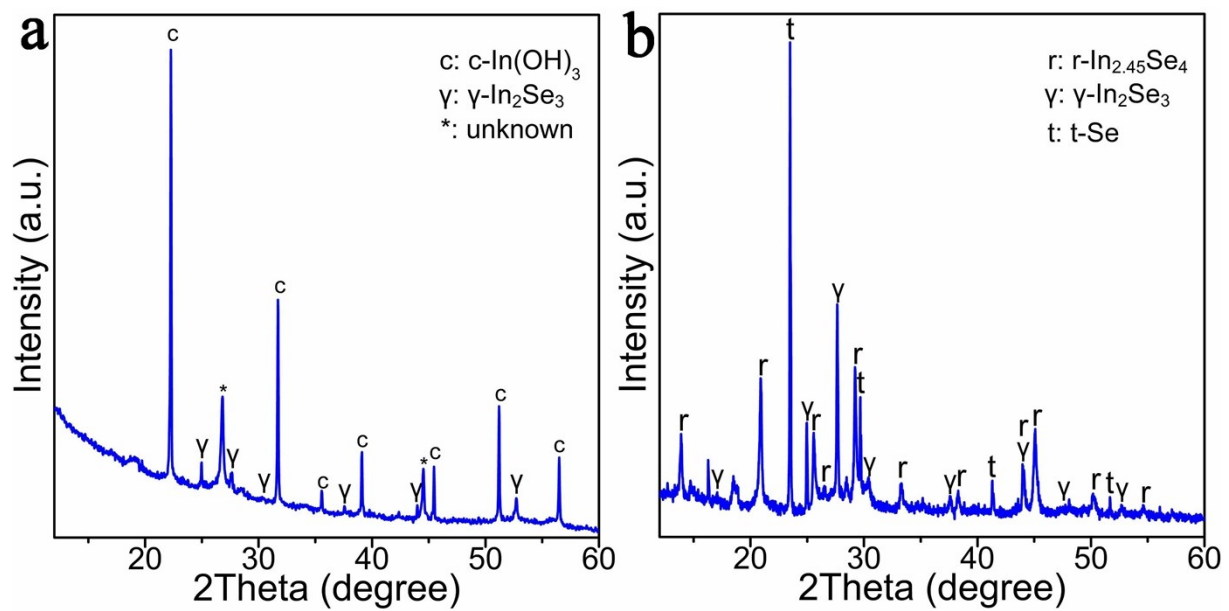


Fig. S6 Lab-based PXRD patterns (Cu K α radiation) of products synthesized with different EDTA/InCl₃ molar ratios: (a) 0, (b) 3.6.

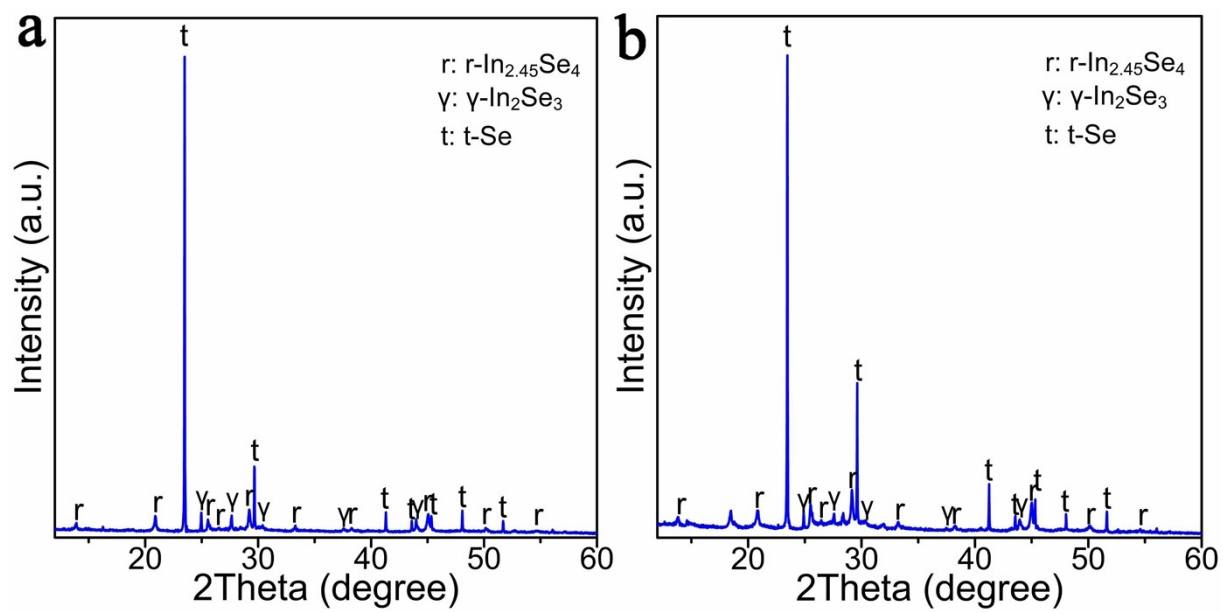


Fig. S7 Lab-based PXRD patterns (Cu K α radiation) of products synthesized at different reaction durations: (a) 6 h, (b) 12 h.

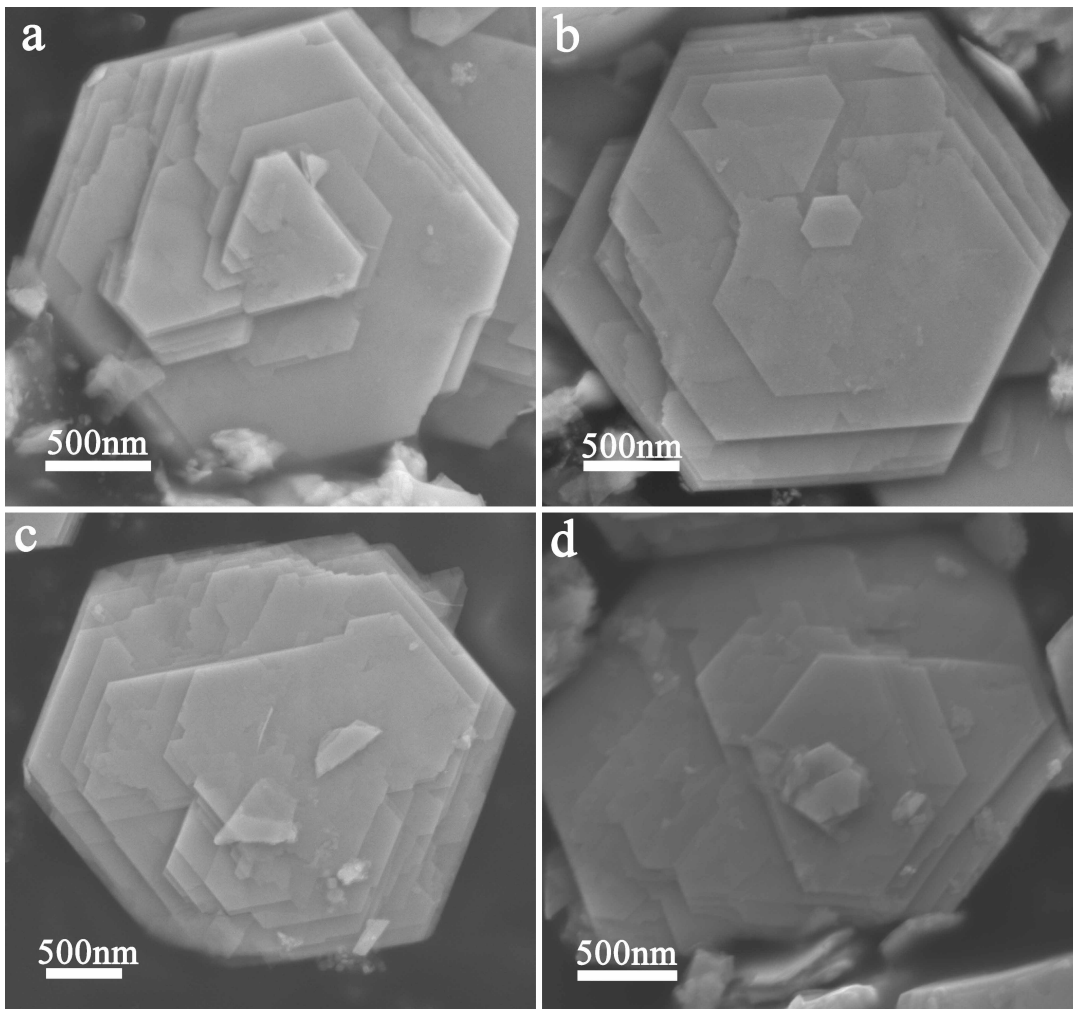


Fig. S8 SEM images of $\text{In}_{2.45}\text{Se}_4$ hexagonal nanoplates.

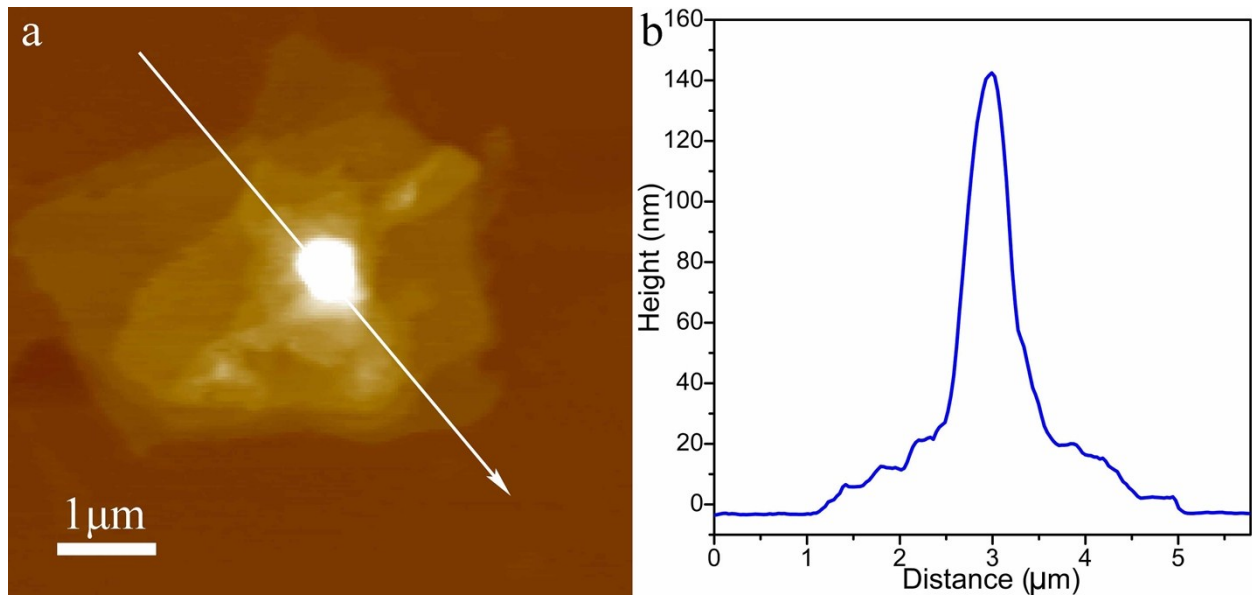


Fig. S9 AFM analysis of $\text{In}_{2.45}\text{Se}_4$ stacked nanoplates: (a) AFM image, (b) height profile from the AFM line scan shown in (a).

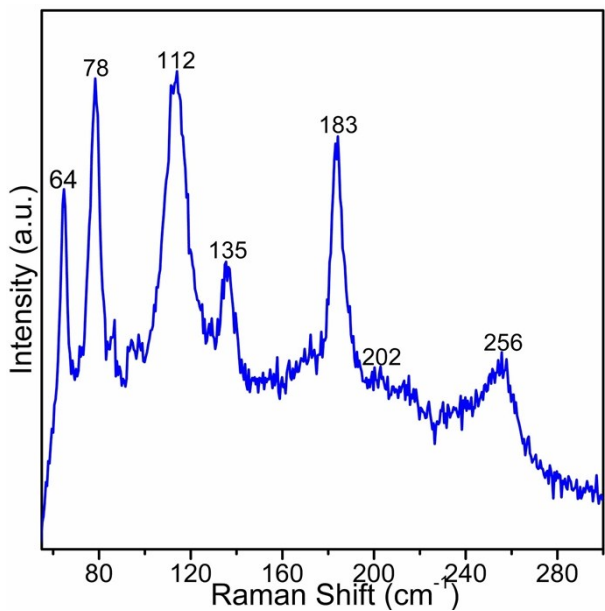


Fig. S10 Raman spectrum of $\text{In}_{2.45}\text{Se}_4$ hexagonal nanoplates.

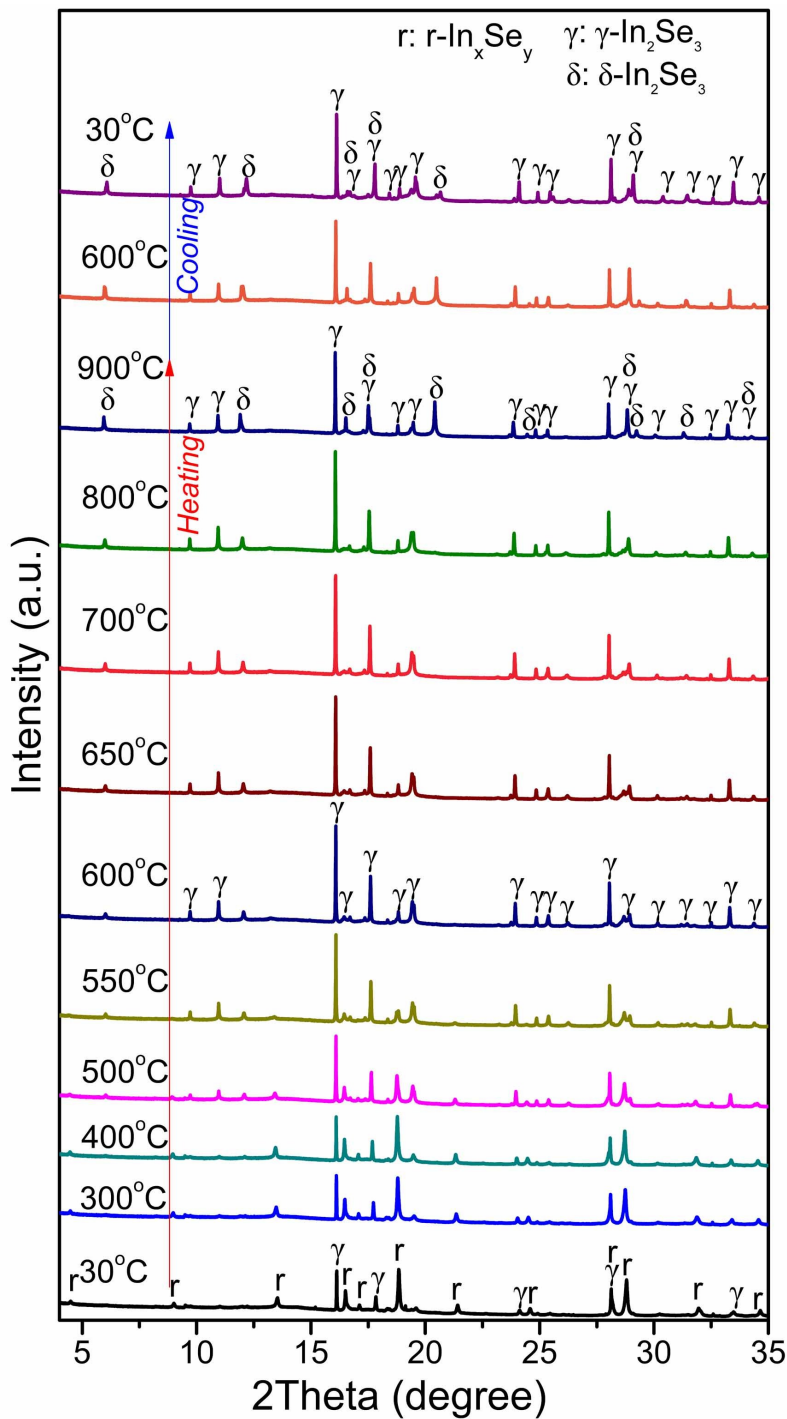


Fig. S11 *In-situ* high temperature synchrotron PXRD patterns of $\text{In}_{2.45}\text{Se}_4$ nano/micro-structures. The X-ray wavelength is 1.0000 Å.

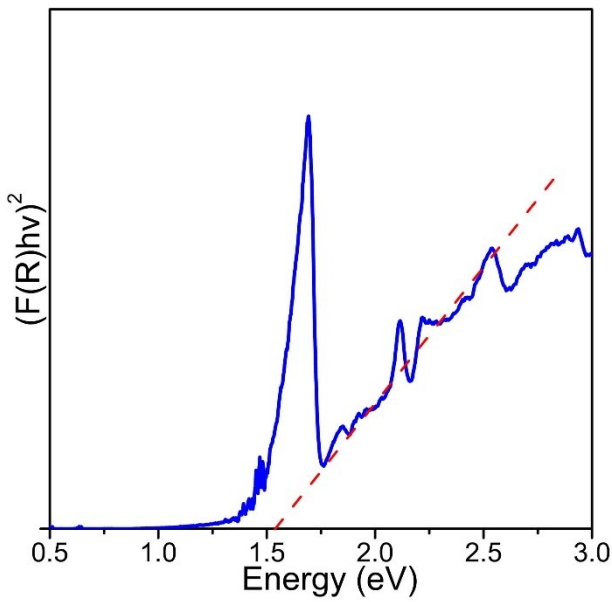


Fig. S12 $(F(R)hv)^2$ vs energy plot from diffuse reflectance spectroscopy data for $\text{In}_{2.45}\text{Se}_4$ nano/microstructures (the peak at 1.4 eV was caused by changing the lamp source during measurement). The direct optical bandgap was determined by taking the tangent to the point of inflection of the plot and measuring the intercept on the x -axis.

Table S1 Crystallographic data of modified In₃Se₄ (space group: *P31m*, *a* = 6.963 Å, *c* = 38.131 Å)

Site	Wyckoff	Symmetry	x	y	z	Occupation
Se1	1a	3m	0	0	0.13070	1
Se2	1a	3m	0	0	0.29480	1
In3	1a	3m	0	0	0.42100	1
Se4	1a	3m	0	0	0.86930	1
Se5	1a	3m	0	0	0.70520	1
In6	1a	3m	0	0	0.57900	1
In7	1a	3m	0	0	0	1
Se8	1a	3m	0	0	0.46403	1
Se9	1a	3m	0	0	0.62813	1
In10	1a	3m	0	0	0.75433	1
Se11	1a	3m	0	0	0.20263	1
Se12	1a	3m	0	0	0.03853	1
In13	1a	3m	0	0	0.91233	1
In14	1a	3m	0	0	0.33333	1
Se15	3c	m	0	0.66666	0.79737	1
Se16	3c	m	0	0.66666	0.96147	1
In17	3c	m	0	0.66666	0.08767	1
Se18	3c	m	0	0.66666	0.53597	1
Se19	3c	m	0	0.66666	0.37187	1
In20	3c	m	0	0.66666	0.24567	1
In21	3c	m	0	0.33331	0	1
In22	3c	m	0	0.66666	0.66667	1
Se23	2b	3	0.33333	0.66667	0.46403	1
Se24	2b	3	0.33333	0.66667	0.62813	1
In25	2b	3	0.33333	0.66667	0.75433	1
Se26	2b	3	0.33333	0.66667	0.20263	1
Se27	2b	3	0.33333	0.66667	0.03853	1
In28	2b	3	0.33333	0.66667	0.91233	1
In29	2b	3	0.33333	0.66667	0.33333	1
Se30	3c	m	0.66667	0.66667	0.13070	1
Se31	3c	m	0.66667	0.66667	0.29480	1
In32	3c	m	0.66667	0.66667	0.42100	1
Se33	3c	m	0.66667	0.66667	0.86930	1
Se34	3c	m	0.66667	0.66667	0.70520	1
In35	3c	m	0.66667	0.66667	0.57900	1